(rec'd. 3-12-80 from SDB)

SURVEY OF RESAMPLING TECHNIQUES USING MSS AND SYNTHETIC IMAGERY

U.S. GEOLOGICAL SURVEY

EDC DOCUMENT 0044

UNITED STATES
DEPARTMENT OF THE INTERIOR
GEOLOGICAL SURVEY
EROS DATA CENTER

SURVEY OF RESAMPLING TECHNIQUES USING MSS AND SYNTHETIC IMAGERY

By Brian P. Bauer

EDC Document #0044

Approved by: Larry L. Metz
Chief, Systems Development Branch

Date: 2/15/80

Sioux Falls, South Dakota

February 1980

SURVEY OF RESAMPLING TECHNIQUES USING MSS AND SYNTHETIC IMAGERY

1.0 Abstract

The objective of this survey is to investigate the methods of interpolation and deconvolution for image restoration The methods evaluated are nearest neighbor, bilinear interpolation, cubic convolution, and two-dimensional deconvolution. The effects of these restoration methods are demonstrated using Landsat multispectral scanner (MSS) data and synthetic imagery.

The effect of these restoration methods are compared as to resolution and spatial frequency effects. The edge effect, a situation that occurs when fill (non-image) data is interpolated with image data, is also addressed.

2.0 Introduction

This survey is written to document and identify the inaccuracies in the MSS data caused by restoration methods. These inaccuracies are manifested by overshoot of intensity values at the edge of image and fill data. The report will also demonstrate the effect on spatial frequency that occurs in an image due to the various restoration methods. The possibility of a radiometric error arises when the pixel position is identified and the improper intensity may be assigned to that pixel. In order to properly address the possibility of a radiometric error, it is important to know the sources of other errors affecting the MSS.

Because the MSS is a scanning system and not an imaging system such as the Return Beam Vidicon (RBV) sensor, there are other corrections done to the imagery before resampling that can contribute significantly to the total image output error. These effects are discussed in Section 3.0.

MSS input data to this survey is prepared by Lyndon Oleson of the Computer Services Branch. Mr. Oleson has implemented a process on the Burroughs 6700 which includes two of the techniques of resampling addressed in this paper.

3.0 Technical Discussion

3.1 Sources of MSS Errors

Adjustments of the image data are used to compensate for radiometric distortion or errors in assigning pixel intenstiy and error in relative pixel positions. In overlaying an image pixel with an absolute ground pixel (56 m x 79 m in area), there are a number of errors that can occur prior to those due to resampling. These errors are listed in Table 1.

Resampling is the process used to determine the radiometry of a pixel location that is established via a geometric correction process. However, since an error in radiometric approximation may misclassify a pixel as part of the surround instead of the target or vice versa, the resampling process can produce a cumulative geometric error as well.

The errors listed in Table 1 are those associated with geometry. It is assumed that the errors listed in Table 1 are removed via the geometric correction process (the determination of a pixel location) prior to resampling. A description of the errors is given below.

The principal error sources are attitude and altitude. The major effect of these errors is scale distortion. Essentially, uncorrected data would have a worst case error of 49.37 km or greater. In actual experience the error in the uncorrected imagery is on the order of 300 m. These geometric distortions are apparent in an uncorrected image when ground features are altered or deformed. Once ground control points (GCP's) are applied to these images, the distortions can be removed. A GCP is a physical feature

Table 1: MSS Data Error Sources and 3σ Magnitudes

(from Ferneyhough, 1977)

Distortion Source	Error, 3σ (km)
Platform:	
Altitude	1.50
Attitude	
Pitch	12.0
Roll	12.0
Yaw	2.46
Pitch Rate	0.93
Roll Rate	0.54
Yaw Rate	0.04
Scan Skew	0.08
Velocity	1.50
Scene:	
Earth Curvature	0.75
Earth Rotation	13.30
Map Projection	3.70
Sensor:	
Mirror Sweep	0.37
Scene/Sensor:	
Panoramic Distortion	0.12
Perspective Distortion	0.08
Total	49.37 km

in a scene whose geodetic location and elevation are precisely known. GCP's are utilized because spacecraft attitude is not precisely determined from the image or ephemeris data. Without GCP's, the data can be system corrected to at least 150 m. With the application of GCP data, this error can be reduced to 50-70 m. However, since the ground control points are derived from say a UTM map at 1:24,000 scale, there are errors of registration in the data due to the application of the GCP's. Estimates of these errors, as a function of the GCP library, are in Table 2.

The distortions due to the UTM projection are maximum at the zone edge of the equator. Therefore, with ground control, it is theoretically possible to reduce MSS errors from a minimum of 150 m to 92.4 m given the nominal resolution of 79 m x 79 m. The published resolution of MSS data is 56 m by 79 m. This is accomplished by over-sampling. Each output image pixel is created from six input pixels and is resampled to a 56 m by 79 m resolution.

Each detector oversamples the ground pixel (Figure 1) in the cross-track direction. This oversampling produces the effective 56 m by 79 m (along and across track) resolution.

In Figure 2 is a description of image data path. The sampled output data $f_r(x)$ is a convolution of input image $f(x)$,

$$f_r(x) = f(x) \times R(x) \qquad (1)$$

where $R(x) = g * (x) + n(x)$. Because of orbit, spacecraft, and sensor anomalies, the set of output data, $f_r(x)$, are never at the locations required by the observer. To correct the data to these output locations, it is required that a warping or mapping function be applied. The GCP's found in the input image are used to generate the mapping function which is a transformation from the geodetic location to the position in the image.

Table 2: Errors in application of GCP library

Error Source	Value (m)
UTM Map (1:24,000	7.4
UTM Measurement	5.0
Total	12.4

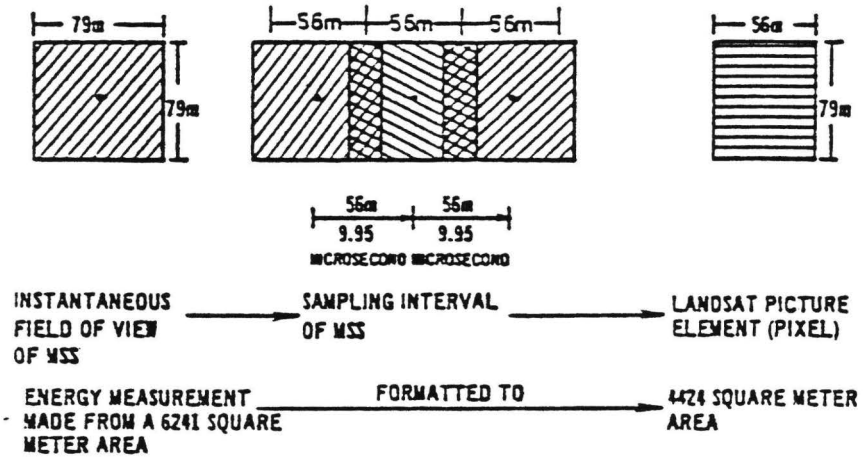

Figure 1: Formation of the MSS picture element. PAO Number: E-6188-35.

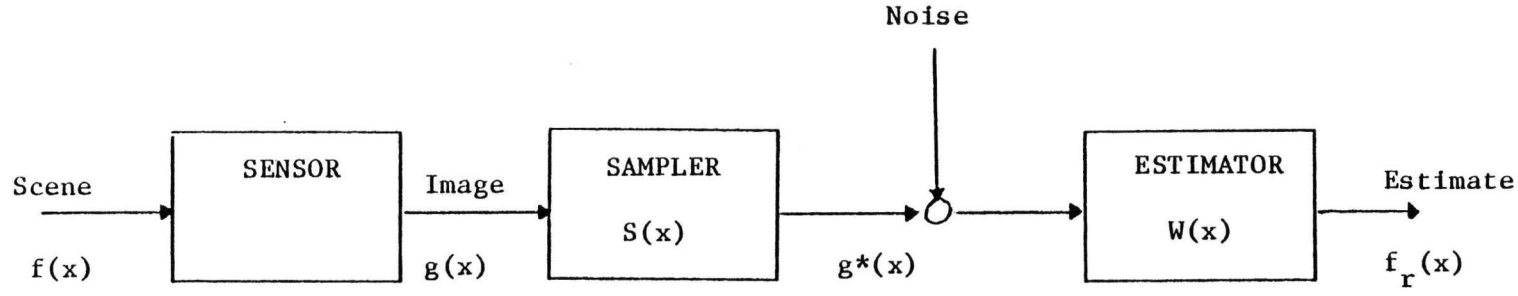

Figure 2: Sensor data path

Raw MSS data is radiometrically corrected for sensor gain and offset. The image (A data) is then reprocessed to a P type image via ground control point information. The application of ground control point information to the data identifies an output pixel in terms of its location in the input (A data). This essentially completes the output pixel process. The output pixel location is often a fraction of the pixel location of the input data. The network of corrected image points are output in a grid. Not all points of an output image are mapped. The grid is constructed so that all points interior to four corner points can be interpolated. The output locations are a specific grid for each cartographic projection. The data is then resampled via nearest neighbor, cubic convolution, or some other method to the new pixel locations.

The sampler in Figure 2 is the resampling function applied to g(x) or A data in the MSS example in Figure 2 and the output is $g^*(x)$.

If f(x) is a band limited signal, then $f_r(x)$ can be obtained by using a sinc function such as $SIN\pi x/\pi x$. If the function g(x) is sampled at least two samples per cycle at the highest frequency, then the restoration is perfect (Hamming, 1977).

A continuous image is reproduced from input image pixels by an interpolator or filter. g(x) is the system impulse response or point spread function, and using (1) in two dimensions,

$$f_r(x,y) = f(x,y) \times g^*(x,y) + n(x,y) \qquad (2)$$

If there is no spectral overlap, then f(x,y) can be made equal to $f_r(x,y)$. This is the same situation where a band limited image can be reconstructed by resampling if the sampling period is less than equal to 1/2 period of the smallest detail in the image. The oversampling of the MSS accomplishes this effect and MSS can be considered a band limited signal.

Likewise, an image signal is band limited if its Fourier transform is zero wherever f(x) or f(y) is greater than some ω. That is, the signal damps to zero at frequency greater than ω. ω is the bandwidth (Duda, 1973) cutoff frequency. If the signal is perfectly band limited at ± ω, then convoluting the point spread function (PSF) with the sampled signal will restore the signal perfectly. The more points that are sampled within the PSF, the better the estimate the restored signal is of the original. The PSF is two-dimensional in that it exists in the along track (x) and across-track (y) directions (Figure 3).

3.2 Resampling Process

The function of resampling is to apply the geometric correction coefficients to the actual input data and to warp an image to a grid of some projection. Typically, a correction to the warped image is accomplished by fitting a polynomial to the horizontal and vertical grid lines and then computing the value of the output intersections from the fitted polynomial (Figure 4).

Once grid points are identified in the input space and in map (or projection) space, a warping function is applied to the input. Not all points of the input space are located in the output space. At a minimum, the corner points only could be selected and used as control points for the warping process. The input space is then resampled at the output point location. The warping process is generally a two-phase procedure. First, the coordinate point or interpolated point is determined for the corrected pixel. Second, the image amplitude at the interpolated point is estimated by resampling the neighbor pixels. This estimated value is then assigned to the corrected pixel. In theory, the optimal interpolator is the sinc function for band limited signals. However, due to reasons described below, the sinc function is not optimal in a time constrained environment.

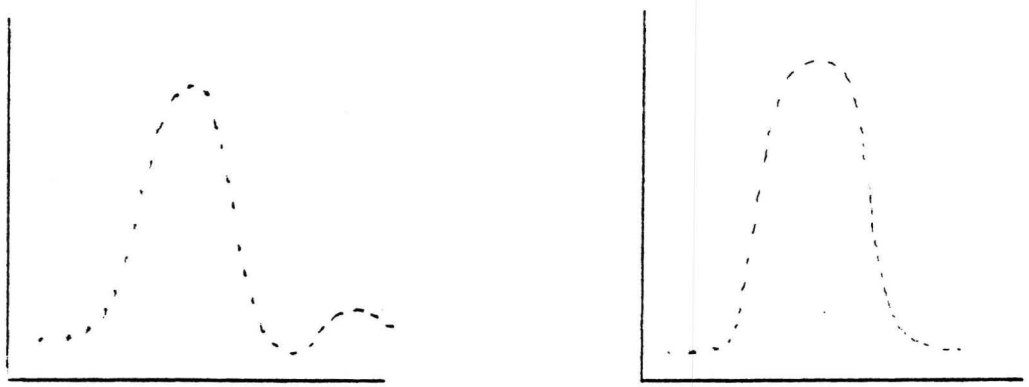

Figure 3: Point spread functions

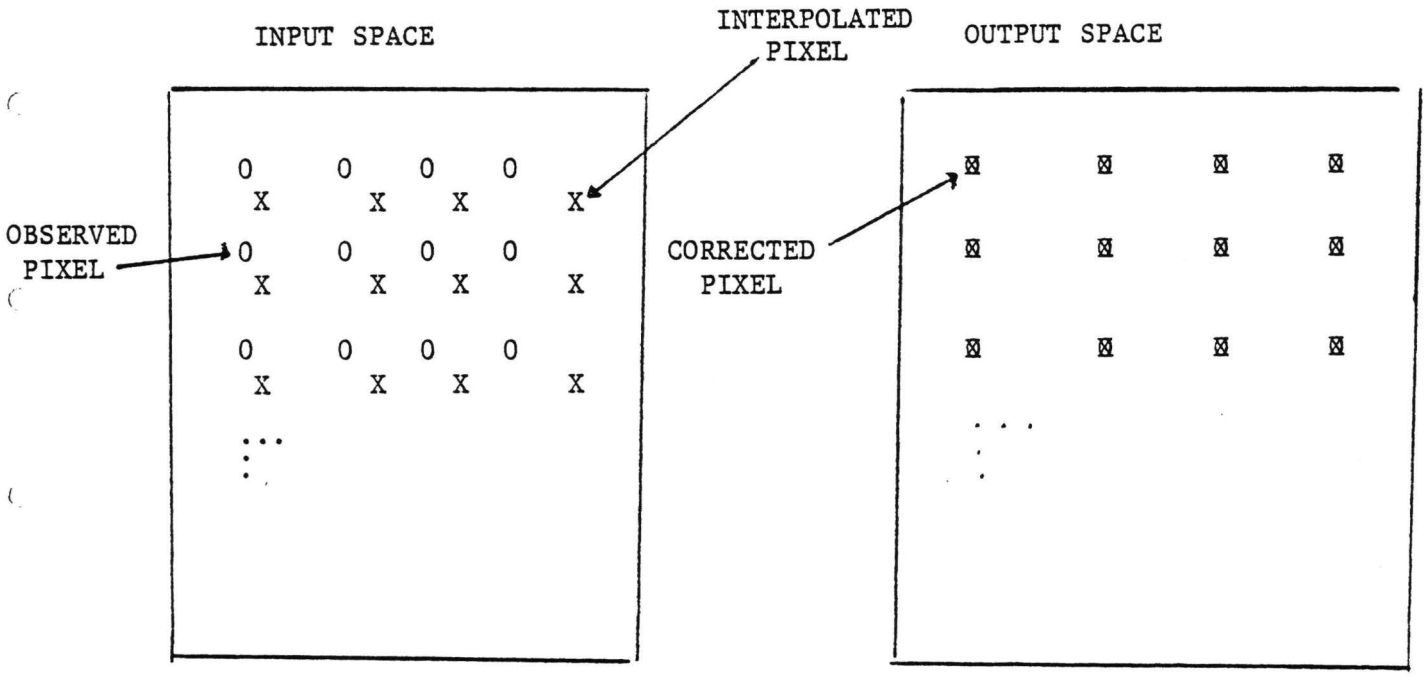

Figure 4: Spatial warping process

One of the problems in constructing the optimum restoration filter, the sinc function, is the estimate of the point spread function. The PSF function is needed to compute the inverse of the sensor processing function on the input data. Because of the quantization noise in the data, it is not necessarily sufficient to estimate the PSF from the data. For MSS data, most researchers report that estimating the PSF from MSS data is highly suspect (McGillem, 1976). Also, the sinc function is not practical to implement because it decays to zero too slowly. For these reasons, deconvolution techniques have not been generally accepted for restoration. The more heuristic methods such as cubic convolution, bilinear, and nearest neighbor are commonly applied.

One of the first reports of application of interpolation techniques to MSS data came from Sam Rifman (Rifman, 1973) of TRW. At approximately the same time, R. Bernstein of IBM made a similar report to NASA as part of the image processing facility proposal for Landsat data processing (Figure 5).

3.3 Literature Review of Resampling Studies

The cubic convolution methods proposed by IBM and TRW are both approximations of the sinc function $\mathrm{Sin}\pi x/\pi x$ (Figure 6). Certain boundary conditions are applied to the TRW and IBM versions to satisfy slope and brightness value continuity restrictions. It is also necessary that the function is symmetric about $x = 0$ and that it damp to zero when $x \geq 2$, as well as at integral multiplies of the sampling interval.

The one-dimensional interpolation is as follows:

$$f(x) = h_1 f_8 + h_2 f_9 + h_3 f_{10} + h_4 f_{11}$$

where $h_1 = h(x+1)$

$h_2 = h(x)$

$h_3 = h(x-1)$

$h_4 = h(x-2)$

(according to TRW)

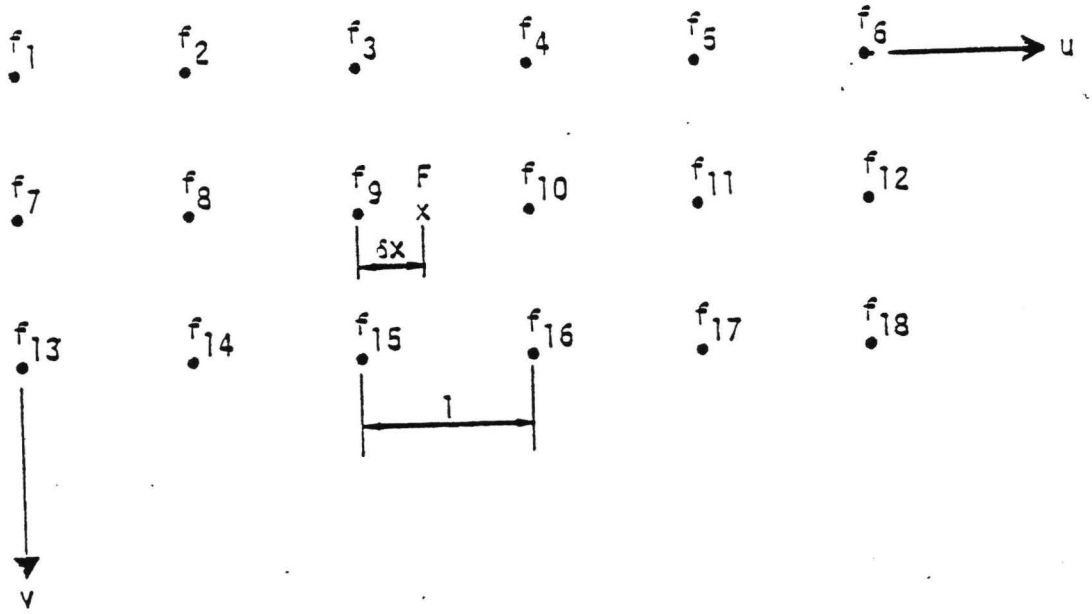

Figure 5a: Along-scan interpolation of pixel F

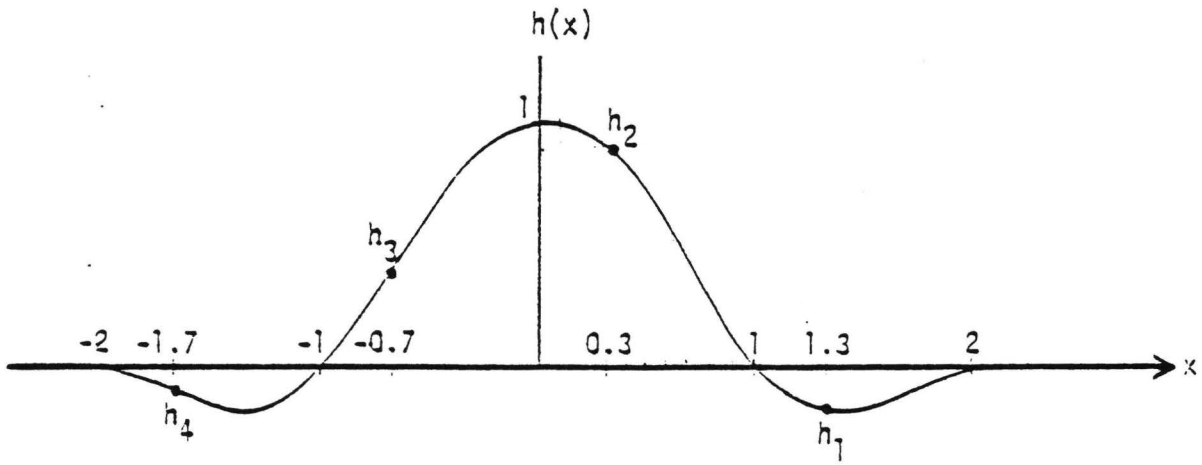

Figure 5b: Weight values for four-point interpolation
A value of $\delta x = -0.3$ is assumed.

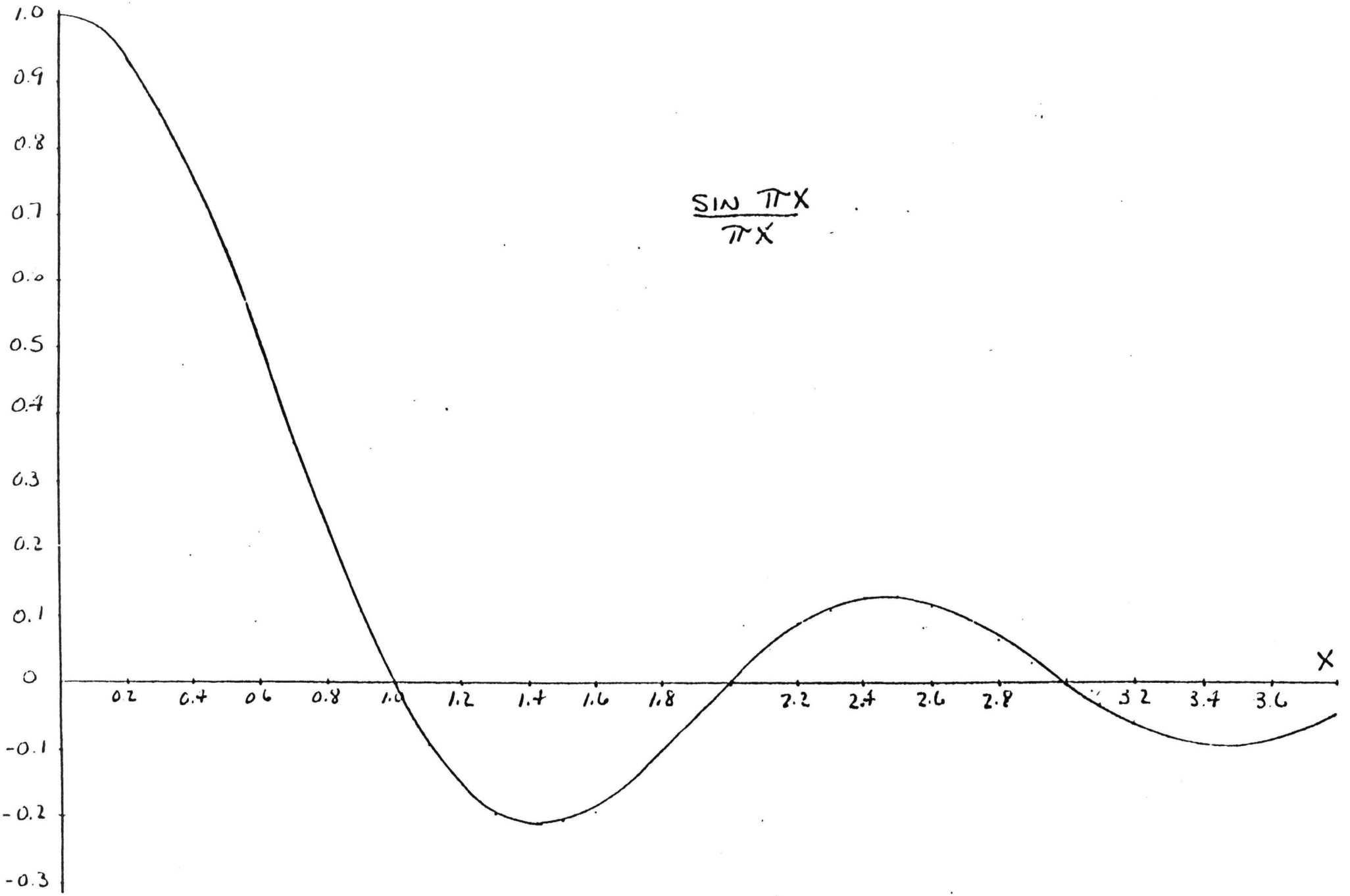

Figure 6: Sinc function

The IBM approximation to the sinc function is the cubic convolution (CC). It is as follows (in one dimension):

$$f(x) = f_0[4-8(1+x) + 5(1+x)^2 - (1+x)^3] + f_9[1-2x^2 + x^3] + f_{10}[1-2(1-x)^2 + (1-x)^3] + f_{11}[4-8(2-x) + 5(2-x)^2 - (2-x)^3] \quad (4)$$

The TRW cubic is expressed:

$$f(x) = X^3 - 2X^2 + 1 \qquad 0 \leq x \leq 1 \quad (5)$$

$$f(x) = -X^3 + 5x^2 - 8x+4 \qquad 1 \leq x \leq 2 \quad (6)$$

$$f(x) = 0 \qquad x \geq 2 \quad (7)$$

This is a spline function with explicit boundary conditions. The nearest neighbor (NN) method is:

$$f(x) = \begin{cases} f_9 \text{ if } x < .5 & (8) \\ f_{10} \text{ if } x \geq .5 & (9) \end{cases}$$

The bilinear (BL) in two dimensions is:

$$f(x,y) = f_6 + x(f_{10} - f_6) + y'* [f_7 + x(f_{11} - f^7) - f_6 - x(f_{10} - f_6)] \quad (10)$$

According to IBM and TRW, their 3-term approximation to SINπx/πx or the sinc function comes closest to being the optimal restoration function. However, all investigators agree that a 20-term sinc function will give the best results.

One of the side effects of an improper resampling function is loss of image resolution and introduction of high spatial frequency artifacts. If only slow changes in the image occurred and the sampling frequency were high enough, no image smear or blurring would occur in both the along and across track directions (Figures 7a and 7b). Thus the requirement would not be for an interpolator, but a sampler since the scene would be over-represented.

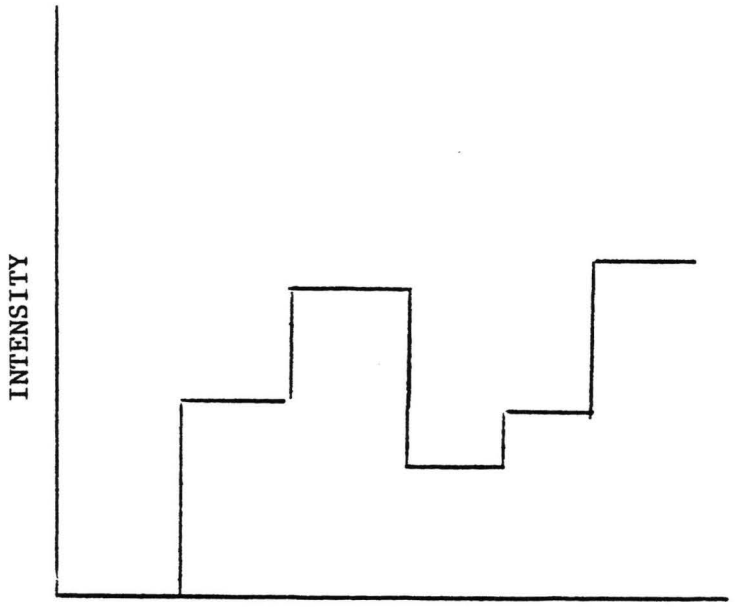

Figure 7a: Input signal

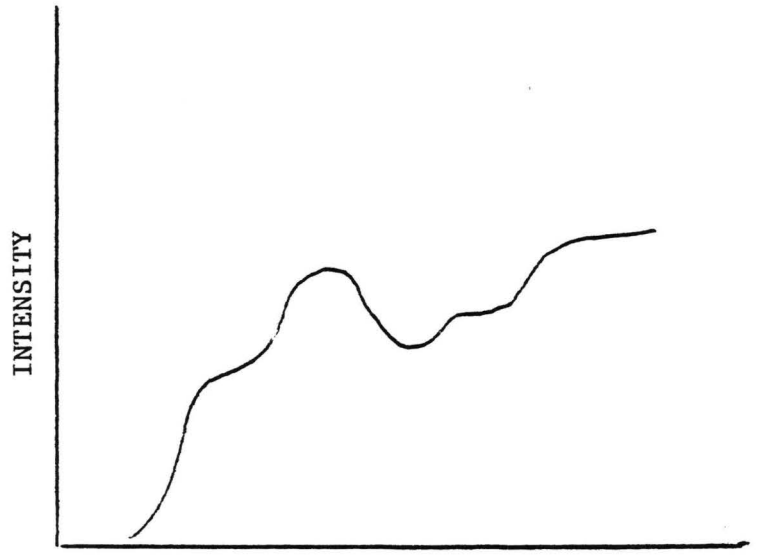

Figure 7b: Output signal

Due to the low spectral power of high frequencies, they can be blurred by resampling techniques in spite of their importance to visual information content. In Figure 8 are the results of applying the above described techniques.

CCRS (Seymour Shlien) uses a 14-point interpolator which is essentially a set of spline functions that are members of the cubic convolution interpolators (similar to the TRW approach):

$$F(x) = d\text{-}x^3 - (1+d)\ x^2+1 \qquad 0 \leq x \leq 1 \qquad (11)$$

$$F(x) = (d-2)\ \ (x^3-5x^2+8x-4) \qquad 1 \leq x \leq 2 \qquad (12)$$

$$F(x) = 0 \qquad x > 2 \qquad (13)$$

$$F(-x) = F(x) \qquad (14)$$

The splines are chosen so that the derivative is zero at (x = -n, n), thus avoiding a first order discontinuity.

3.4 Optimal Restoration Techniques

At the present time, R. Dye at ERIM has been experimenting with two-dimensional deconvolution. Essentially, he suggests that the above mentioned methods tend to widen the point spread function of the data and are equivalent to convolving the data twice, thus lowering the resolution. He also asserts that these techniques severely impact classification efforts.

The method of two-dimensional deconvolution rests on the ability to adequately model the PSF.

$$f_r(x) = f(x) \times g^*(x) \qquad (15)$$

f(x) is the original scene and g*(x) is the PSF.
The PSF is determined from the blur circle and detector size in cross scan direction. This technique essentially tries to take the sensor effect out of the imagery.

Currently, experiments with the deconvolution technique are ongoing at CCRS, USDA, and EDC. Although it will be addressed later in Section 3.7, most

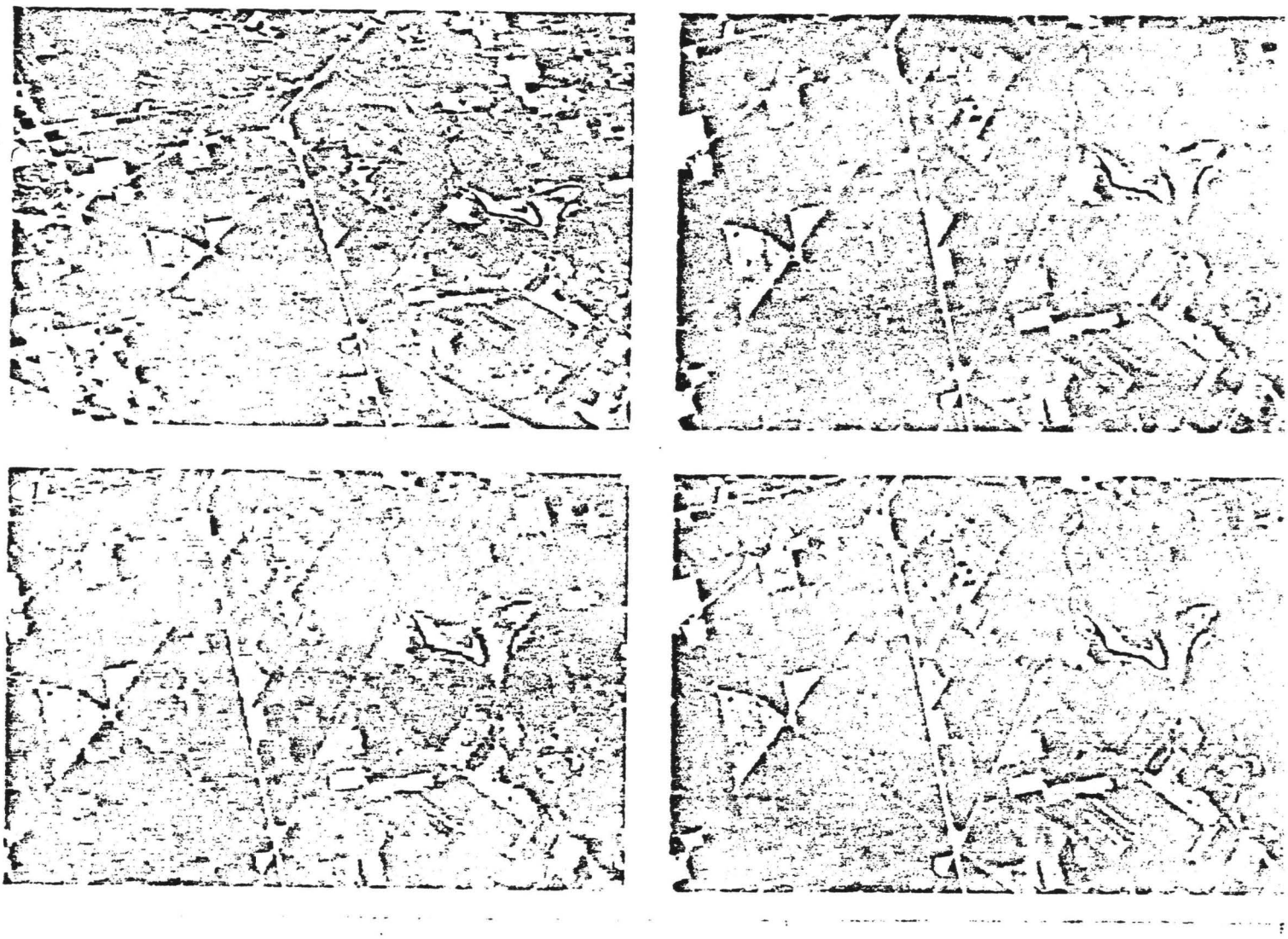

Top Left - Original Data

Bottom Left - Nearest Neighbor Resampling

Top Right - Bilinear Interpolation Resampling

Bottom Right - Cubic Convolution Resampling

Figure 8: Resampling results on ERTS MSS subimage

techniques of interpolation other than nearest nighbor take a considerable amount of computer time. Indications are that 2-D deconvolution takes substantially longer CPU time than cubic convolution.

Sensor output $f_r(x,y)$ is essentially a convolution of the sensor $S_I(x,y)$ with the input data $F_I(x,y)$.

$$F_p(x,y) = S_I(x,y) \times F_I(x,y) \tag{16}$$

$$F_R(x,y) = F_p(x,y) \times R(x,y) \tag{17}$$

What ERIM is suggesting is that they can estimate a deconvolution function $S^{-1}(x,y)$ such that

$$S^{-1}(x,y)\ F_p(x,y) = \hat{F}_I(x,y). \tag{18}$$

where $\hat{F}_I(x,y)$ is an estimate of $F_I(x,y)$.

3.5 Resampling Effects on Classification Accuracy

To date, there is not a lot of conclusive work on the effect of resampling techniques on classification accuracy. Most of the techniques described, work better in some situations and not so well in others. In a study at EDC concerning the accuracy of classification (Nelson, 1978), it is stated that there is no significant difference in the classification accuracy for a maximum likelihood classifier.

In Table 3 are the statistics from the test MSS scene. The means and standard deviations do not appear different. However, looking at specific islands in the MSS imagery used in this study, a number of interesting results are apparent. In the original data, four islands are apparent. They are also apparent in the NN image. However, after CC and BL, the four islands are smoothed to three. This can be seen by computing the area of islands: the number of pixels making the southern most island in the original image is 9. However, in the NN, BL, and CC image, this islands contains 16, 17, and 19 pixels respectively. Investigators such

Table 3: Resampled Data

METHOD	BAND	RANGE	Vr	MINIMUM	MAXIMUM	MEAN	STANDARD DEVIATION
NN	1	69	1	15	84	29.999	9.869
	2	83	4	5	88	11.989	7.694
	3	78	4	2	80	7.204	6.767
	4	62	2	0	62	3.634	6.119
BL	1	66	4	15	81	30.000	9.782
	2	79	8	5	84	11.988	7.599
	3	72	10	2	74	7.213	6.661
	4	56	8	0	56	3.635	5.982
CC	1	71	1	15	86	30.002	9.886
	2	86	1	3	89	11.991	7.718
	3	79	3	0	79	7.195	5.791
	4	60	4	0	60	3.625	6.146
Original Data	1	70	6	15	85	28.904	12.026
	2	87	13	5	92	10.085	5.236
	3	82	17	2	84	5.439	3.837
	4	64	14	0	64	2.292	3.418

as Bob Dye maintain that deconvolution techniques will overcome these smoothing effects. This affect is a degradation in resolution. The average intensity value is shown in Table 4. In Table 5 are the results of the maximum likelihood classifier on the resampled data. It is obvious in this example that there is not much difference between the classifier performance on this data. One problem with this example is that approximately 94% of the data is water. A similar test over cultivated or cultural areas would be more instructive.

Using synthetic imagery, the effects of resampling on slanted and vertical edges with various starting samples (Figures 9a, 9b, and 9c) were investigated. Various distances, d, were used to look at interpolated sample effect. The interpolation point is the $\underline{x}$ in the original imagery. As can be seen in Figure 11, CC can cause edge under and over shoot (see also Figure 10). In Figure 9, the only edge that would remain correct after interpolation is $\underline{b}$. The other edges, $\underline{a}$ and $\underline{c}$, are not translationally invariant after resampling.

Various estimates of error in Figure 11a and 11c have been made for interpolators. One such set of data (Beaudet, 1976) is given in Table 6.

Another example of the edge effect of interpolators is found in Figure 11. This data shows the effect of CC on MSS A data to produce P type data. The input data is 12 pixels by 8 lines of MSS A data. The 127 count values are fill pixels. The first line of data which is 0 0 0 46 46 46 becomes 127 127 127 127 127 48 after CC interplation in this example.

Another example of the effect of resampling on imagery is in Table 7 which describes the effect on MSS of CC to the peak value in the histogram.

The percent occurrence of the most frequently occuring value is reduced in each case. In fact, the reduction ranges from 6 to 12% for band 7

Table 4: Island statistics (from Nelson, 1978)

Island	# pixels	μ	σ
Original	9	15	2.9
NN	16	14.8	2.8
BL	17	14.4	2.7
CC	19	15.2	3.9

Table 5: Percent scene classifications (from Nelson, 1978)

Percentage of Points/Group			
Deep Water	24.3	25.8	24.2
Medium Water	42.8	37.1	42.8
Shallow Water 1	14.3	14.4	15.1
Shallow Water 2	10.5	13.7	9.6
Shallow Water 3	1.7	2.3	2.0
Vegetation	2.3	2.2	2.6
Bright Vegetation	3.6	3.6	3.3
Sparse Vegetation	.2	.7	.3
Sand	.2	.2	.2

10	0	0	0	0	0	0	0	0	0	0	10
0	10	0	0	10	10	10	10	0	0	10	0
0	0	10	0	0	0	0	0	0	10	0	0
0	0	0	10	0	0	0	0	10	0	0	0
a				b				c			

Figure 9: Synthetic edge orientations

					INTERPOLATION METHOD					
					Cubic		Bilinear		Nearest	
Image					(.5,.5)	(.3,.3)	(.5,.5)	(.3,.3)	(.5,.5)	(.3,.3)
10	10		10	10	8	9	10	10	10	10
20	10	x	10	10	12	12	13	12	10	10
10	20	x	10	10	18	29	15	16	20	20
10	10	x	20	10	12	12	13	12	10	10
10	10	x	10	20	8	9	10	10	10	10
10	10	x	10	10						
127	127		50	50	89	104	89	104	50	127
127	127	x	50	50	89	104	89	104	50	127
127	127	x	50	50	89	104	89	104	50	127
127	127	x	50	50						
127	50	x	50	50	40	39	50	50	50	50
127	50	x	50	50	40	39	50	50	50	50
127	50	x	50	50	40	39	50	50	50	50
127	50	x	50	50						
127	127		127	50	137	132	127	127	127	127
127	127	x	127	50	137	132	127	127	127	127
127	127	x	127	50	137	132	127	127	127	127
127	127	x	127	50						

d x - interpolated pixel

Figure 10: Summary of interpolation effect for varying d on synthetic imagery

A EDGE

0	0	0	46	46	46	48	51	46	48	48	46
0	0	0	49	47	47	49	47	47	49	49	49
0	0	0	48	46	48	48	48	48	46	50	50
0	0	0	50	50	48	48	50	50	50	50	50
0	0	0	47	49	47	49	51	49	49	49	51
0	0	0	50	48	48	48	48	48	48	45	48
0	0	0	48	46	51	51	46	48	48	48	51
0	0	0	47	49	45	45	49	47	49	51	49

P EDGE

127	127	127	127	127	48	46	49	50	49	49	49
127	127	127	127	127	47	47	49	49	47	47	49
127	127	127	127	127	46	47	48	48	48	45	45
127	127	127	127	91	50	48	46	47	47	47	47
127	127	127	127	38	51	47	46	47	47	49	51
127	127	127	127	45	45	46	47	47	49	50	49
127	127	127	127	45	42	45	48	46	46	45	47
127	127	127	127	47	47	47	48	47	45	44	48

Figure 11: Image edge for A and P data

(.8 - 1.1 μm) and band 6 (.7 - .8 μm). Note also the increased spread around the peak. The spread of data increased about 6% for all bands.

3.6 Errors in Landsat Imagery as a Result of Resampling

An IBM report concludes (Ferneyhough, 1977) that CC definitely can cause overshoot or higher contrast relative to the surround. It may also cause spread or smear. This effect is more severe in the along track than in the across-track direction. However, CC also removes discontinuities due to offset and sample delay. In areas of near uniform radiance, the differences caused by CC are minimal, and in fact, a certain amount of noise reduction can result (see Table 6).

As we have stated above, the sinc function is optimal, however, it is not feasible to implement because of slow decay time. CC produces no staircasing or discontinuities in the data. NN however has an error of at most ± 0.5 pixels due to sample spacing. This discontinuity is the result of its zeroth order interpolation. BL (using 4 pixels as input) causes resolution degradation due to truncation of peak intensities (see Table 7). This in effect is a smoothing process of the high spatial frequencies.

In Figure 12 is a comparison of the intensity error in an MSS scene for the types of resampling presented. For the larger number of counts, CC gives the lowest error. For small intensity errors though, the CC method is highest and NN is the lowest.

3.7 Timing Considerations

On an IBM 370/155, the times recorded to process three MSS images can be seen in Table 8. Jayroe doesn't state what CPU his work was done on, but the times are quite different. Whereas Jayroe reports a 4 to 1 difference between CC and NN, Bernstein reports a 31 to 1 difference.

Table 6: Percent error as a function of resampling method

Percent Error	Method
10	Truncated SinπX/πX
50	NN
50	BL
23	CC

Table 7: Effect of cubic convolution on peak histogram value

	Band	BV Peak	% of Scene	BV Range	% of Scene	% Reduction of Peak Value
A	4	23	4.1	17-30	43.5	10
P	4	23	3.7	17-30	39.9	
A	5	21	4.3	17-30	39.1	10
P	5	21	3.9	17-30	36.0	
A	6	38	3.4	37-45	37.7	6
P	6	38	3.2	37-45	35.0	
A	7	44	2.6	34-47	32.8	12
P	7	44	2.3	34-47	30.2	

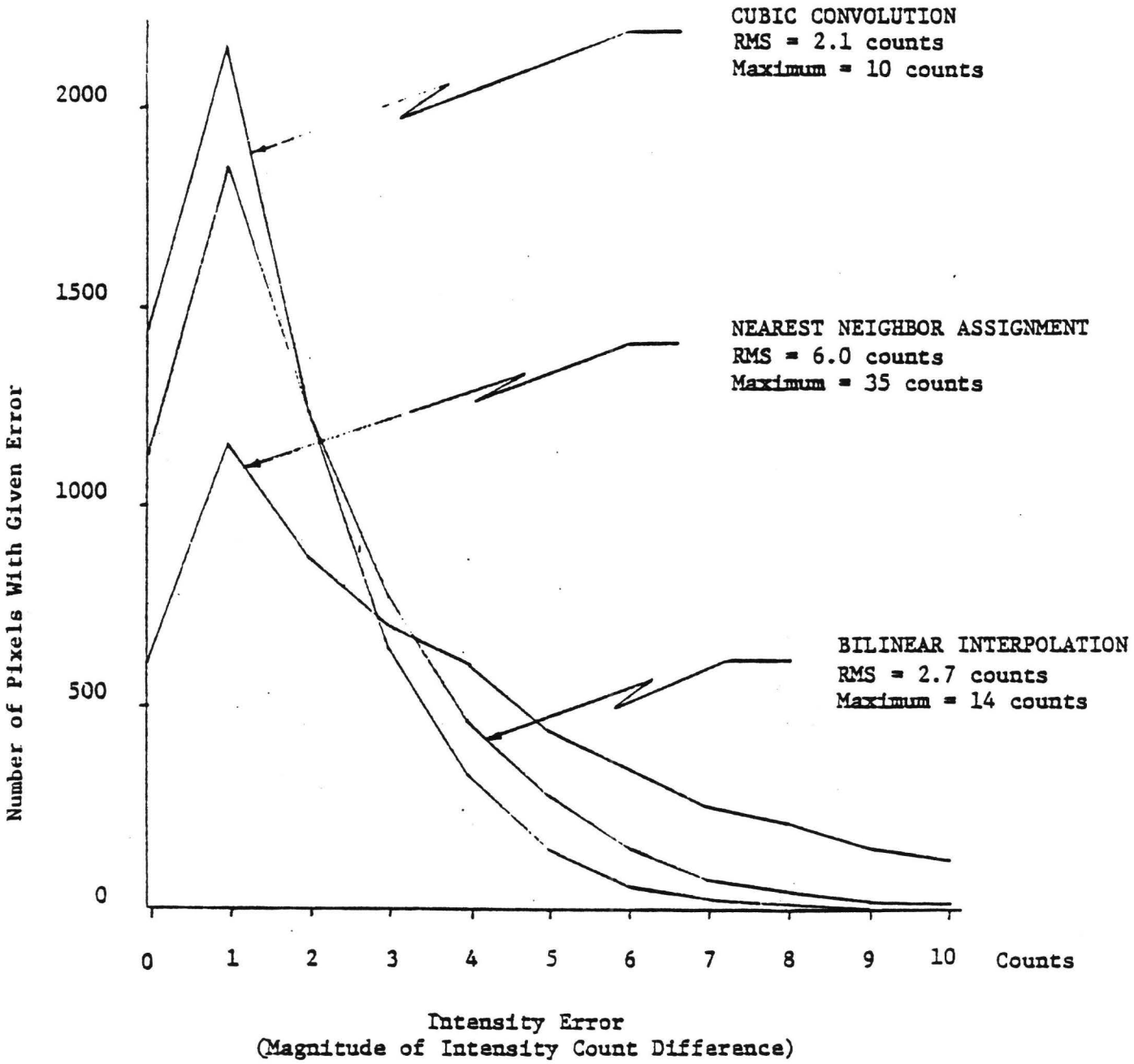

Figure 12: Resampling error histograms - natural image (Bernstein, 1975)

Table 8: Timing (Jayroe/Sec.)

Resampling Technique			Timing (sec.)
NN	1	34.8	160 (53) 1
BL	2	59.6	216 (720) 13
CC	4	135.5	4980 (1660) 31

4.0 Summary and Future Work

Most of the work that was reviewed pointed out that NN changed the histogram the least, whereas BL and CC changed it the most. In most cases, the modes would shift around, whereas the means of data would remain pretty much the same. Also, a change in the variance would occur as a result of which method was chosen (see Table 9). In fact, the variance is reduced as we implement the higher order resampling methods.

Primarily, the most important effect that can be measured of the various interpolators is what sort of effect they have in image classifiers. However, evaluation of this effect is complicated by the fact that most of this information is scene dependent. That is, performance of one classifier might be improved for one technique, but would not be optimal for all scenes. As long as scenes are made up of a few large homogeneous areas, the type of resampler probably is not too important. However, when you are investigating boundary conditions or transition areas between two or more areas, there is a potential for misclassification. Essentially, this is the reason that the Corps of Engineers (McKim, 1979) while utilizing MSS data, classifies the uncorrected data before the correction and interpolation process.

Therefore, as far as future work is concerned, classification results should demonstrate the error between the original and the resampled image in the transition areas as opposed to comparing the resampling techniques among themselves as a function of classifier performance. The potential for interpolation techniques acting as filters to smooth natural discrimination in the original data and to affect change detection and multi-temporal classification should also be investigated.

Table 9: Effect of various resampling techniques on scene statistics (from Jayroe, 1974)

	Band 4			
	Raw	NN	BL	CC
Mode	30.00	30.00	28.00	28.00
Mean	30.24	30.27	30.27	30.27
Variance	11.70	8.21	6.46	8.31

In addition to the above, as far as future work on interpolation is concerned, there are a number of important results to look at. Some of these areas to be investigated are:

1. Because resampling results in an increase of the point spread function, thus a decrease in resolution, what is the effect of bi-resampling and what are the optimal resampling techniques for input to the bi-resampling process?
2. Create context dependent interpolators that function on local scene characteristics as opposed to global techniques now used.
3. Develop interpolation techniques that are shape preserving techniques. Presently, the histogram changes very little as a function of shape of interpolator, however, boundaries of objects in the scene do change.
4. Modify CC to account for oversampling in the horizontal direction.
5. What sort of patterns are added to images as a result of resampling? That is, develop a figure of merit for resampling that measures the statistical effect.
6. Quantify the effects of bi-resampling.
7. Modify CC to avoid overshoot at edges.
8. The effect of bi-resampling on bi-resampled data.

Bibliography

Beandet, P. R., 1976, "Context Dependent Interpolation," Image Science Mathematics.

Bernstein, R., 1975, "Digital Pre-Processing of ERTS Imagery," IBM Report NAS5-21716.

Duda, R., 1973, "Pattern Classification and Scene Analysis."

Dye, R., 1976, "Restoration of Landsat Images by Discrete 2-D Deconvolution," ERIM.

Ferneyhough, 1977, IBM Report on Resampling.

Hamming, R., 1977, Digital Filters.

Jayroe, R., "NN, BL, CC Interpolation," NASA TMX-73348.

McGillem, C. D., 1976, "Resolution Enhancement of ERTS Imagery," NAS9-14016.

McKim, Ike, 1979, Private communication.

Nack, N. L., 1977, "Rectification and Registration of Digital Images and the Effect of Cloud Detection," LARS Symposium.

Nelson, C., 1979, "Some Effects of NN, Bl, and CC Resampling on Landsat Data."

Rifman, S., 1973, "Digital Rectification of ERTS MSS Imagery," NASA SP-32-7.

Shlien, S., 1979, "Geometric Correction Registration, and Resampling of Landsat Imagery," CCTS.

Simon, K., "Digital Image Deconstruction and Resampling for Geometric Manipulation."

Taranik, J. V., 1978, "Characteristics of the Landsat Multispectral Data System."